CHAPTER IV
RESULTS AND DISCUSSION

These methodology are applied to case study of complex LNG (multistage cascade cycle) under subambient temperature for minimizing energy requirement which can help to improve the process with minimum work required. In this section, there are three designs.

The example of subambient process for LNG is illustrated. The multistage cascade refrigeration is applied for LNG process. This process consists of three pure refrigerants, methane, ethylene and propane, which have different three boiling points. Fist, natural gas is cooled in propane cycle then it is cooled in ethylene, finally it is liquefied to -155 °C in methane cycle. The multistage cascade has been simulated using commercial software ProII version 9.1. The fluid package chosen to provide thermodynamics properties is Peng Robinson equation of state. The ambient conditions are assumed to be 25 °C (298.15 K) and 1 bar. The LNG composition and other assumption are given in Table 4.1 and natural gas cooling curve is illustrated in Figure 4.1 (Pereira and Lequisiga, 2014). The temperature difference between hot and cold stream is assumed to be 3 °C (Marmolejo-Correa and Gundersen , 2012) because the smaller temperature difference, the smaller exergy destruction.

Table 4.1 The LNG compositions and other assumption

NG temperature	30 °C
NG pressure	40 bar
NG flowrate	450 mmscfd
NG composition	
C1	90
C2	7.32
C3	0.35
iC4	0.00075
nC4	0.0001
iC5	0.04
N_2	2.3
CO_2	0.0005
Compressor and expander efficiency	75 %

The design begins with generating basic diagram as known as CCs including pressure effect and then ECCs are generated with exergy components by commercial software PROII. The initial stream data are shown in Table 4.2. In this case study is presented in which different option for decreasing power consumption.

Table 4.2 Initial stream data of multistage cascade refrigeration of LNG process

	T_s (°C)	T_t (°C)	P_s (atm)	P_t (atm)	ΔH (MMkW)
H11	12.34	-1.36	4.48	4.48	-0.1842
H12	8.6	-1.36	16.5	16.5	-0.0056
H13	30	-1.516	39.47	39.47	-0.0083
H14	35.8	25.43	9.5	9.5	-0.2323
H21	-12.31	-23.57	2.12	2.12	-0.1414
H22	-1.36	-23.63	16.5	16.5	-0.0127
H23	-1.52	-23.57	39.47	39.47	-0.0060
H31	-23.63	-36	16.5	16.5	-0.1223
H32	-24.33	-35.57	6.02	6.02	-0.0035
H33	-23.57	-36.17	39.47	39.47	-0.0036
H41	-35.57	-65.73	6.02	6.02	-0.1002
H42	-36.17	-65.7	39.47	39.47	-0.0104
H51	-75.08	-86.94	2.45	2.454	-0.0344
H52	-41.13	-86.9	35.5	35.5	-0.0205
H53	-65.7	-86.98	39.47	39.47	-0.0315
H61	-86.9	-90.57	35.5	35.5	-0.0307
H62	-86.98	-90.11	39.47	39.47	-0.0040
H71	-89.09	-125.21	9.402	9.402	-0.0148
H72	-110.19	-125	3.536	3.536	-0.0003
H73	-90.11	-125	39.47	39.47	-0.0161
H81	-125	-143.65	3.536	3.536	-0.0047
H82	-125	-143.7	39.47	39.47	-0.0070
H91	-143.7	-155	39.47	39.47	-0.0040
C1	-4.36	-4.36	4.08	4.08	0.1981
C2	-26.58	-26.58	1.89	1.89	0.1600
C3	-38.95	-38.95	1.15	1.15	0.1294
C4	-68.7	-68.7	5.37	5.37	0.1106
C5	-89.96	-89.9	2.12	2.12	0.0864
C6	-93.24	-93.24	1.8	1.8	0.0328
C7	-128.21	-128.21	8.15	8.15	0.0312
C8	-146.63	-146.6	2.94	2.94	0.0117
C9	-161.56	-161.56	1	1	0.0039

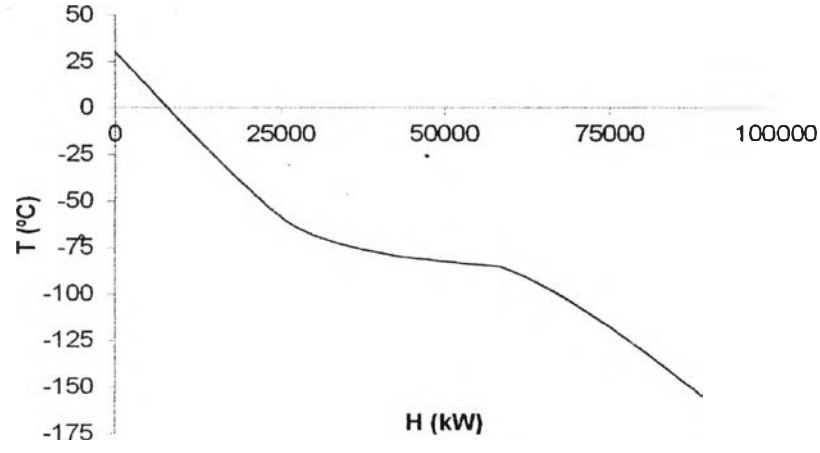

Figure 4.1 Natural gas cooling curve of case study.

4.1 Improved Case by Shaft Work Targeting Technique

The ECCs is applied for shaft work targeting as introduced by Linnhoff and Dhole (1992). The concept of methodology is that replaced the temperature of CCs with Carnot factor, $\eta_C = 1 - (\frac{T_0}{T})$, resulting in ECCs as shown in Figure 4.3 (b). The area between the specific curve and reference temperature line in ECCs illustrates the amount of necessary exergy supply to achieve the target temperature. For cascade in multistream exchanger as shown in Figure 4.2 (a), the reference temperature is temperature that adsorbs heat as shown in Figure 4.2 (b) (dashed line represents hot streams reject heat to cold stream in each exchanger). The real shaft work can be estimated from ECCs which expressed by equation (4.1).

$$W = \frac{\Delta Ex_r}{\eta_{ex}} \tag{4.1}$$

Where ΔEx_r is the theoretical shaft work obtained from ECCs of real refrigeration system, W is the actual work from process by simulation or measurement and η_{ex} estimated shaft work requirement since refrigeration systems and heat exchanger network to process.

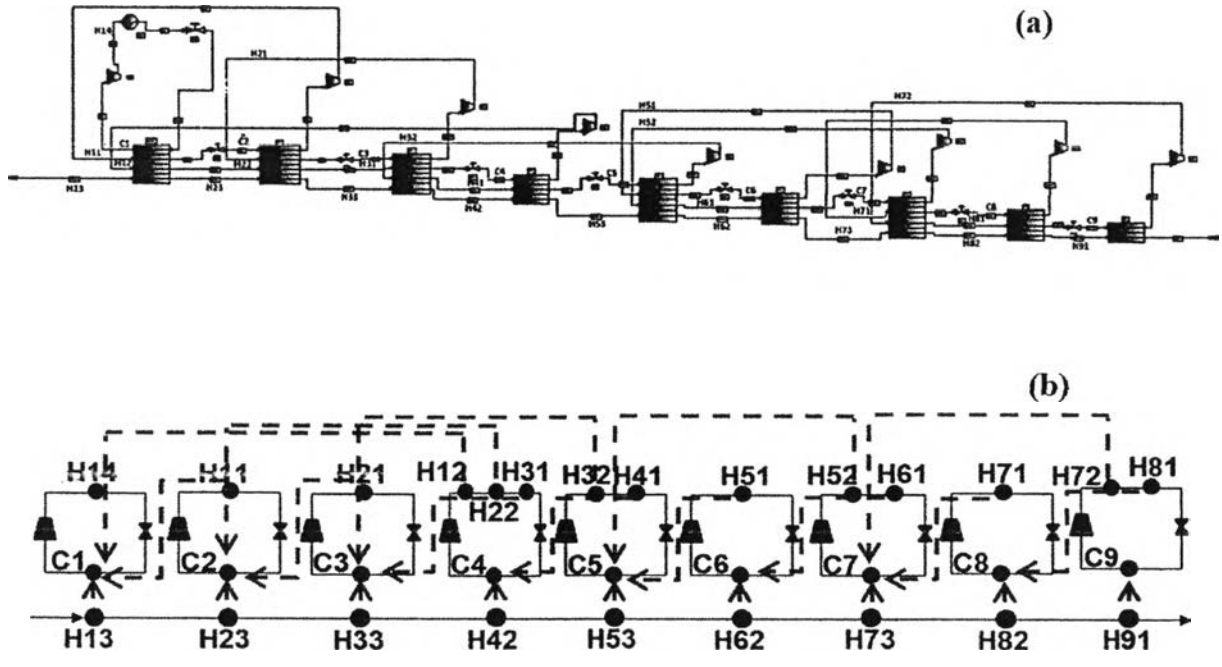

Figure 4.2 (a) Base case multistage cascade refrigeration of LNG process in PROII. (b) Scheme of multistage cascade refrigeration of LNG process.

Figure 4.3 (a) shows the flow diagram of work or exergy losses $(\sigma T_0)_{HEN}$ in which the refrigeration system supply exergy (ΔEx_r) to HEN then HEN supply to process (ΔEx_p). From ECCs in Figure 4.3 (b), ΔEx_r of base case equals to 99,366.76 kW and 39,784.30 kW of $(\sigma T_0)_{HEN}$ lose due to heat transfer. Shaft work from simulation is 144,089.53 kW. The real shaft work can be estimated from ECCs by $W = \frac{\Delta Ex_r}{\eta_{ex}}$ while η_{ex} that equals to 0.68.

To reduce the exergy losses correspond to reduce shaft work, the refrigeration system is improved as shown in Figure 4.4. From ECCs the changed condition of utility help to reduce $(\sigma T_0)_{HEN}$ by changing pressure of cold stream (C9) then the end temperature of cold stream is changed to -158 °C therefore $(\sigma T_0)_{HEN}$ reduce around 39,449.1 kW.

$$\Delta (\sigma T_o)_{HEN} = (\sigma T_o)_{HEN,1} - (\sigma T_o)_{HEN,2}$$
$$= 39{,}784.30 - 39{,}449.1 = 335.2 \text{ kW}$$

The reduction of shaft work can be estimated by

$$\Delta W = \frac{\Delta\,(\sigma To)_{HEN}}{\eta_{ex}} \text{ while } \eta_{ex} = 0.68$$

$$= 492.9 \text{ kW}$$

So that shaft work is reduced to 143,596.56 kW. Comparison between value from simulation and one from this methodology, resulting in Table 4.3.

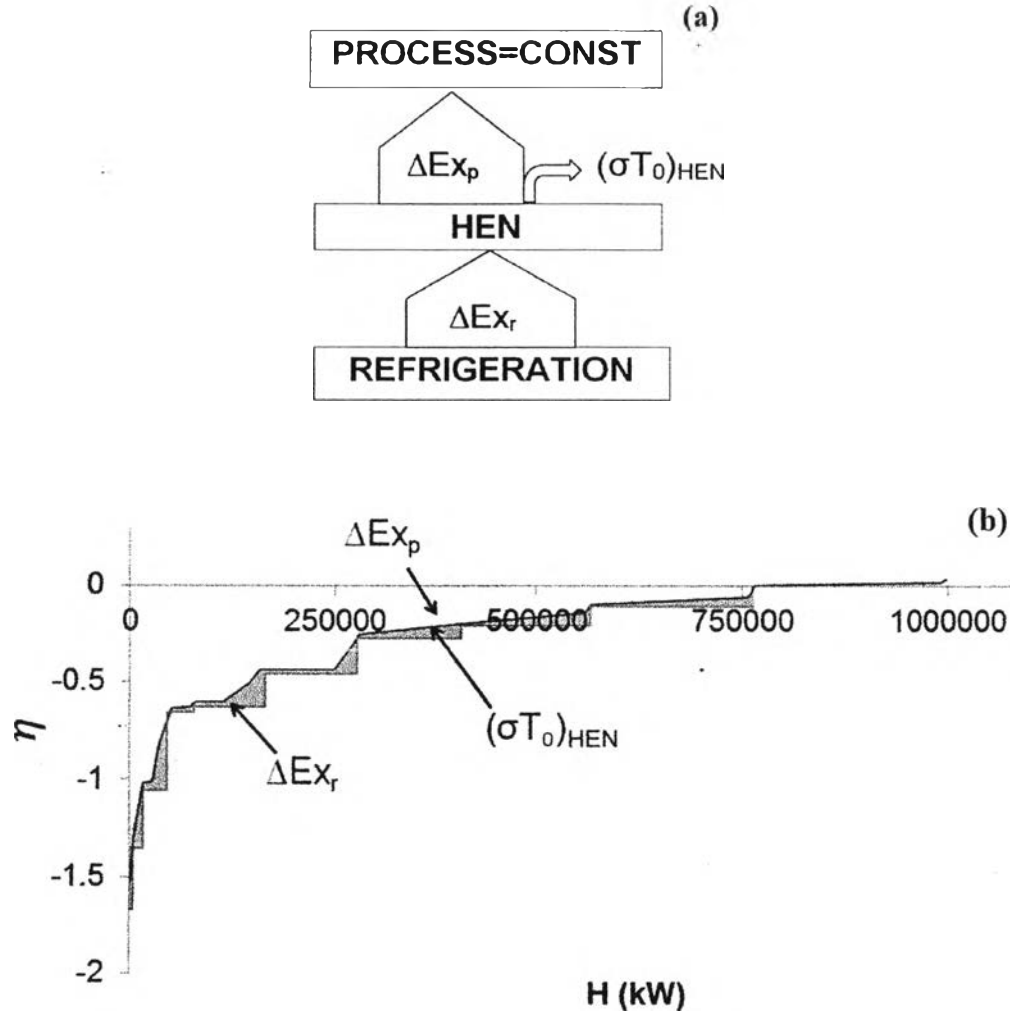

Figure 4.3 (a) The flow diagram of work or exergy losses $(\sigma T_0)_{HEN}$. (b) ECCs of base case multistage cascade refrigeration of LNG process.

Table 4.3 Compared between value from simulation and shaft work targeting

	Base case (kW)	Improved Case (kW)
Simulation	144089.5	143840.9
Methodology	-	143,596.56
Error		0.17%

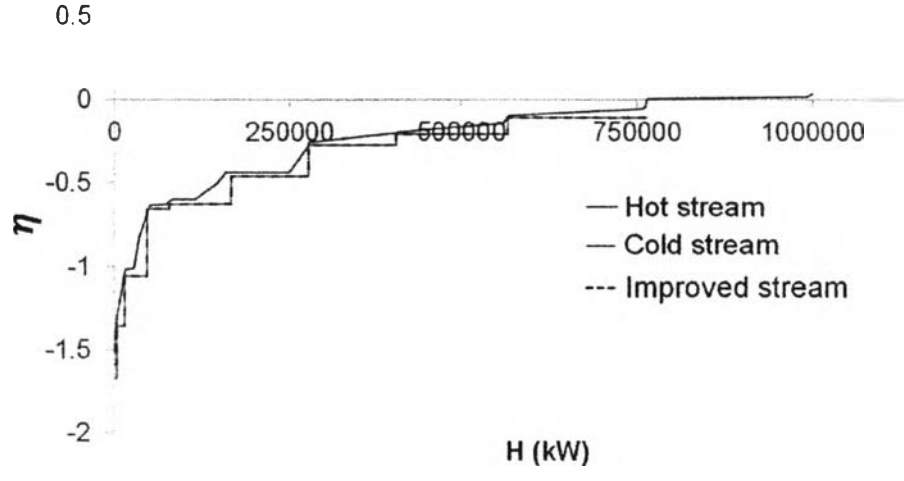

Figure 4.4 ECCs of improved multistage cascade refrigeration of LNG process.

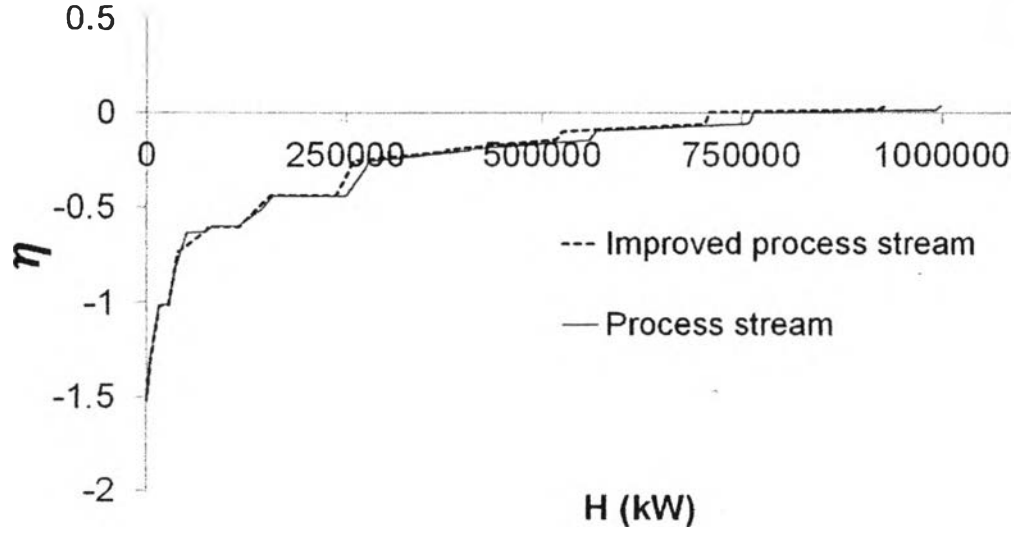

Figure 4.5 Process stream change by using ECCs.

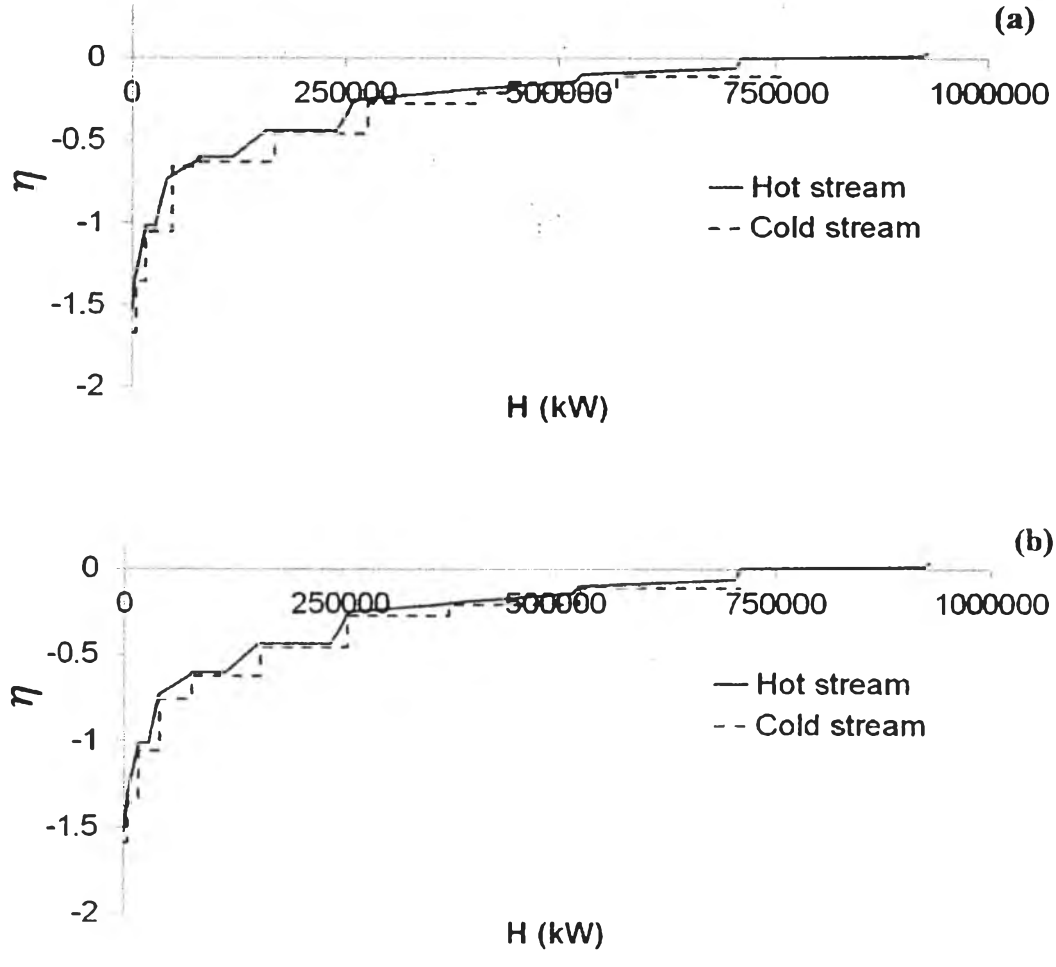

Figure 4.6 (a) ECCs of changed process condition. (b) ECCs of improved cold stream condition.

Next, the change in process condition using the CCs to improve the process is done first. The change of pressure in hot streams affects the shape of hot composite curve. From Figure 4.5 the process stream or hot exergy composite curve is shifted (dashed line) results in reducing the energy consumption. When process is changed, ΔEx_p is reduced so $(\sigma T_0)_{HEN}$ increases as shown in Figure 4.6 (a), we have to shift $(\sigma T_0)_{HEN}$ by changing the level of refrigeration as shown in Figure 4.6 (b). The shaded area will be reduced, resulting reducing shaft work to 127,953.13 kW.

4.2 Improved Case by the Extended Pinch Analysis and Design Methodology and Novel Exergy Diagram

Aspelund *et al.* (2007) proposed the Extended Pinch Analysis and Design (ExPAnD) methodology which combines between Pinch Analysis and Exergy Analysis for minimum external heating, cooling and irreversibility. The use of expander and compressor helps the streams act as utilities. Therefore this methodology is chosen to help to improve process. Starting with base case, the first step estimates the exergy efficiency based on the ratio of total exergy inlet and outlet of streams equals to 97.95 %. The second step performs traditional CCs as shown in Figure 4.7 where 232,600 kW of cold utility as cooling water is required. However 144,089.53 kW of compressor work is required.

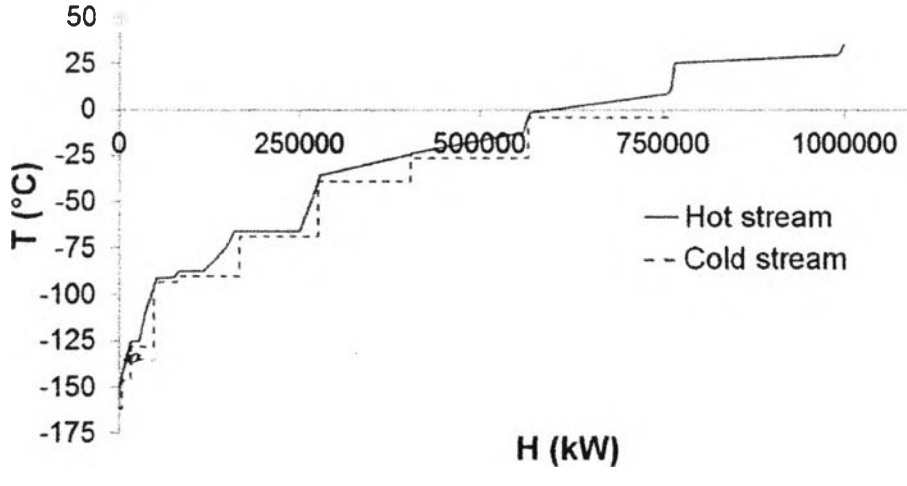

Figure 4.7 CCs of base case multistage cascade refrigeration of LNG process.

Next, process is modified in the third step by selecting heuristic rules (Aspelund *et al.*, 2007) in order to design the process. First, streams in subambient processes with a supply pressure higher than target pressure should be always expanded in an expander. Figure 4.8 shows the process which using expander instead of valve, the need for cold utility is reduced to 210,600 kW. The power consumption is reduced to 131,168.53 kW. The power generation from the expander is 9,423.26

kW. The exergy efficiency of alternative 1A is 98.6 %. When cold stream is expanded to its target pressure of 1 bar prior heat exchanger will give the lowest possible supply temperature by keeping flowrate constant to original value which shown in Figure 4.9. The exergy efficiency of alternative 1B is 98.3 %.

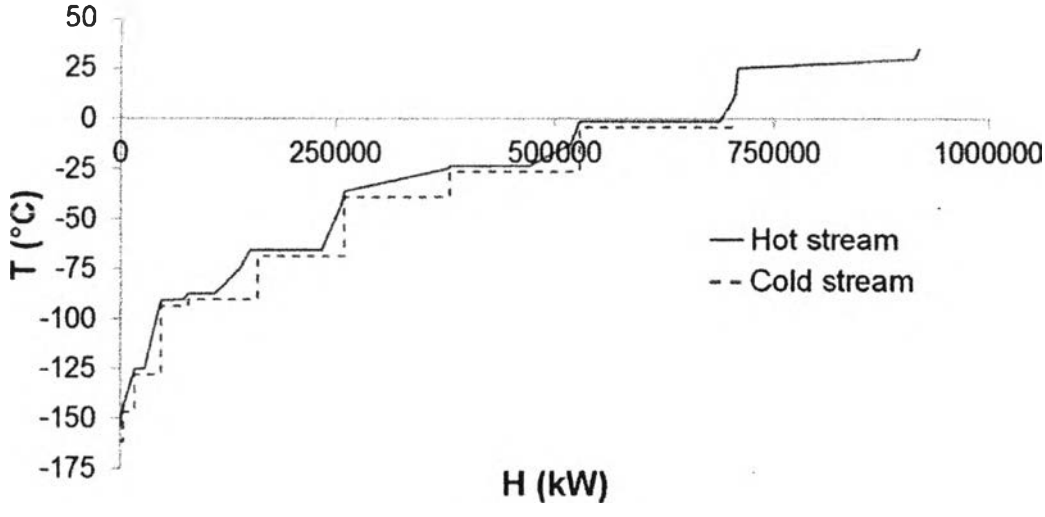

Figure 4.8 CCs of alternative 1A multistage cascade refrigeration of LNG process.

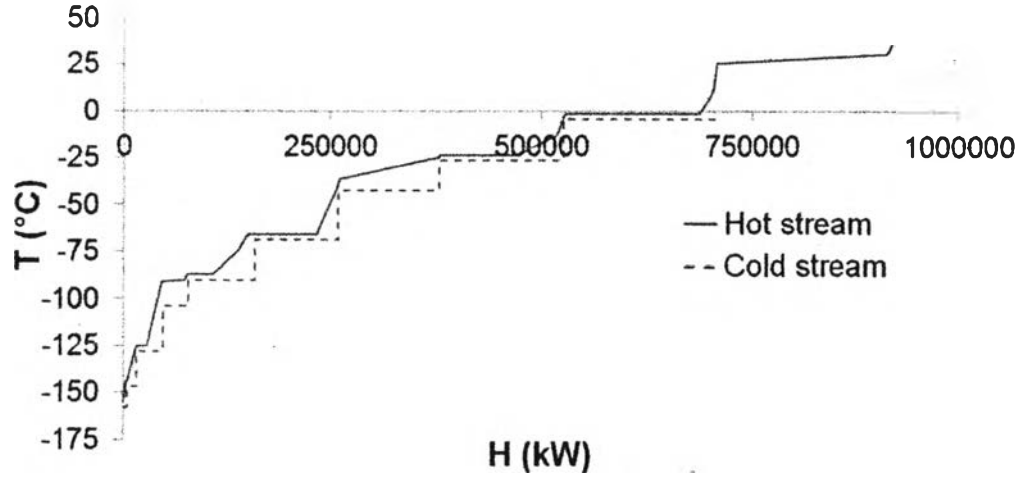

Figure 4.9 CCs of alternative 1B multistage cascade refrigeration of LNG process.

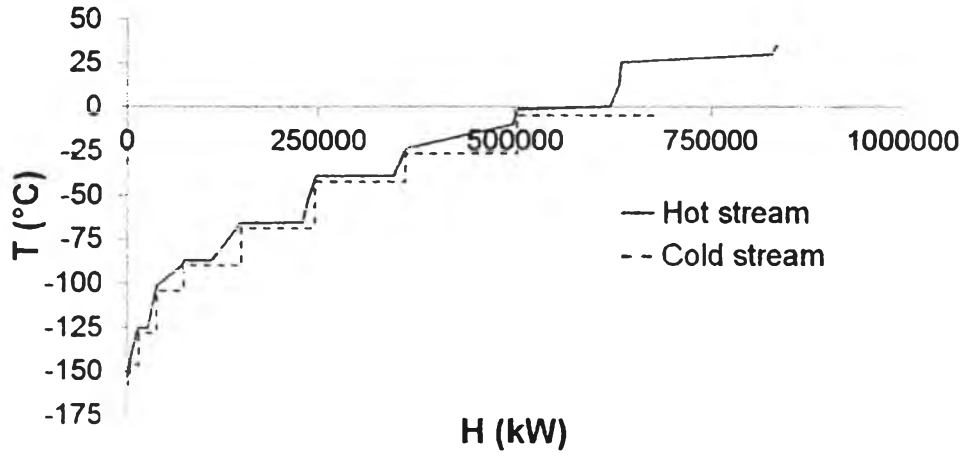

Figure 4.10 CCs of alternative 1C multistage cascade refrigeration of LNG process.

There is room for improvement design, from Figure 4.9 the larger temperature gap between CCs result in unnecessary irreversibility. Moreover, if the pressure of supply stream is higher than target stream, it can reduce cold utility requirements with power generation. So the improvement as shown in Figure 4.10, the required work and cooling duty is reduced to 118,456.83 kW and 200,300 kW respectively. In addition, the generated work is 6,895.24 kW. The exergy efficiency of alternative 1C is 98.4 %.

This section represents the novel exergy diagram which introduced by Marmolejo-Correa and Gundersen (2012) has been used for determining the exergy target with maximizing exergy recovery and minimizing exergy destruction that can be read directly from the graph. This diagram can be used parallel with ExPAnD method to see the reduction of irreversibility or exergy destruction. The diagram start with base case by transforming traditional CCs of base case into exergetic temperature and temperature based exergy diagram which focus on subambient condition by equation (2.75) as shown in Table 4.4 and the overlapping of the end temperature in hot and cold of CCs is transformed to exergetic temperature represents to exergy destruction as shown in Figure 4.11 (a) and (b).

In Figure 4.11 (a) and (b), the exergy destruction is shown by changing the overlapping temperature in CCs to exergetic temperature, it equals to 33,872.57 kW where focus on subambient temperature. Improvement of alternative 1A, the exergy

diagram according to CCs in Figure 4.8 is shown in Figure 4.12, illustrates 29,000 kW of exergy destruction. Next, the exergy diagram of alternative 1B according to CCs in Figure 4.9 is shown in Figure 4.13 which presents 33,000 kW of exergy destruction. After improved process the new exergy diagram according to CCs in Figure 4.10 is shown in Figure 4.14 can be visualized that exergy destruction is reduced to 23,000 kW which reduce by 32 % from base case. This was achieved by using ExPAnD method and manipulating pressure.

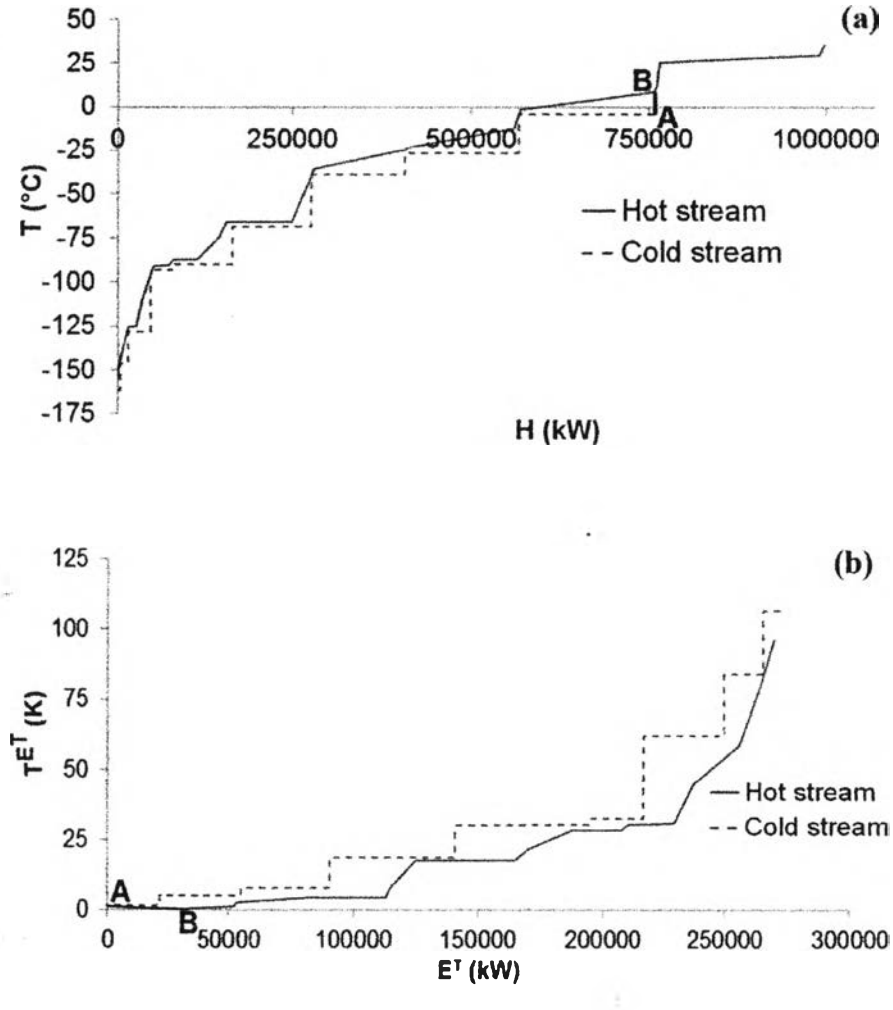

Figure 4.11 (a) CCs for the base case multistage cascade refrigeration of LNG process. (b) Exergy diagram for the base case multistage cascade refrigeration of LNG process.

Table 4.4 Exergy data of base case multistage cascade refrigeration of LNG process

	T_s (°C)	T_t (°C)	Ts^{E^T} (K)	Tt^{E^T} (K)	ΔE^T (MMkW)
H11	12.341	-1.36	0.277	1.238853	0.0176
H12	8.6	-1.36	0.468	1.238853	0.0004
H13	30	-1.516	0.041	1.254032	0.0003
H14	35.801	25.43	0.191	0.00031	-0.0006
H21	-12.311	-23.57	2.549	4.446201	0.0274
H22	-1.36	-23.629	1.239	4.457691	0.0018
H23	-1.516	-23.568	1.254	4.445812	0.0009
H31	-23.629	-36	4.458	7.247687	0.0308
H32	-24.328	-35.571	4.595	7.137826	0.0008
H33	-23.568	-36.173	4.446	7.292265	0.0008
H41	-35.571	-65.734	7.138	17.45577	0.0429
H42	-36.173	-65.7	7.292	17.4409	0.0037
H51	-75.082	-86.936	21.857	28.40325	0.0206
H52	-41.134	-86.9	8.639	28.38162	0.0092
H53	-65.7	-86.98	17.441	28.42971	0.0168
H61	-86.9	-90.571	28.382	30.64586	0.0194
H62	-86.98	-90.114	28.429	30.35752	0.0012
H71	-89.091	-125.209	29.719	58.7295	0.0145
H72	-110.187	-125	44.918	58.5176	0.0003
H73	-90.114	-125	30.358	58.5176	0.0128
H81	-125	-143.649	58.518	79.9807	0.0006
H82	-125	-143.704	58.518	80.05236	0.008
H91	-143.704	-155	80.052	95.98008	0.0057
C1	-4.357	-4.357	1.548	1.547783	-0.0217
C2	-26.58	-26.58	5.054	5.053827	-0.0335
C3	-38.952	-38.952	8.030	8.030296	-0.0353
C4	-68.704	-68.704	18.786	18.78586	-0.0506
C5	-89.962	-89.9	30.262	30.22313	-0.0542
C6	-93.235	-93.235	32.364	6.789869	-0.0215
C7	-128.208	-128.208	61.837	61.83658	-0.033
C8	-146.629	-146.6	83.942	83.90239	-0.0159
C9	-161.563	-161.563	106.456	106.4565	-0.0067

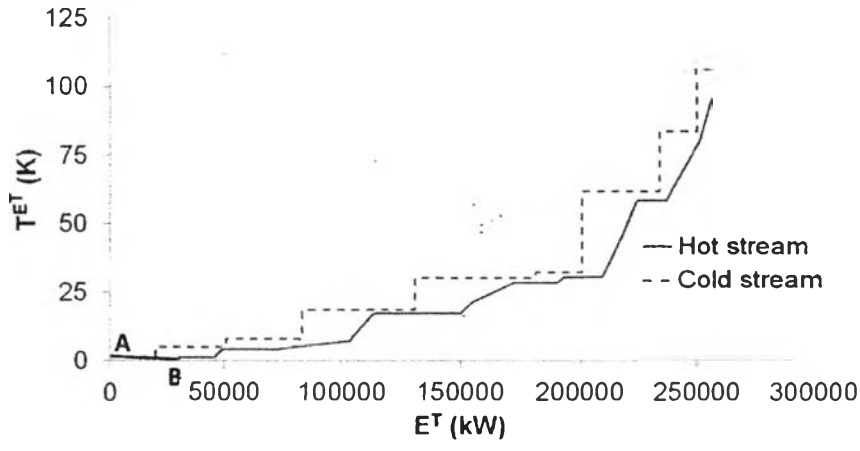

Figure 4.12 Exergy diagram for the alternative 1A multistage cascade refrigeration of LNG process.

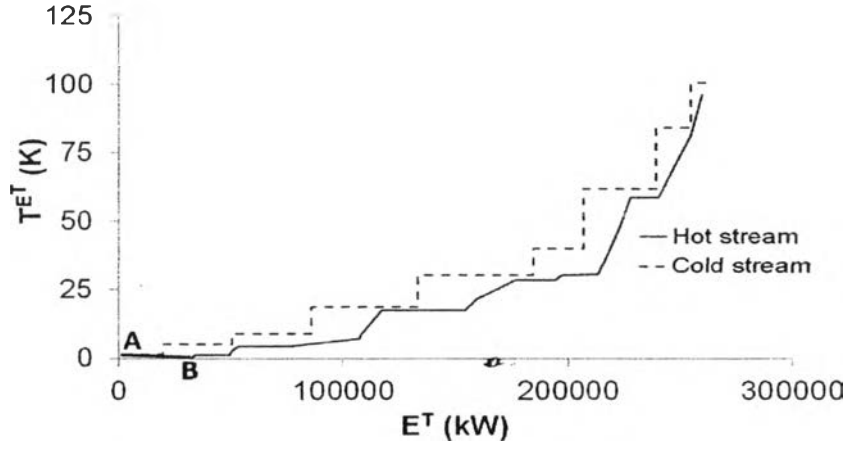

Figure 4.13 Exergy diagram for the alternative 1B multistage cascade refrigeration of LNG process.

The exergy destruction in exergy diagram of base case and shaded area $(\sigma T_0)_{HEN}$ in shaft work targeting (Linnhoff) are validated with and total exergy destruction of LNG heat exchangers in commercial software (ProII) in order to check the accuracy of diagram as shown in Table 4.5 that the exergy diagram is rather explicit for exergy target.

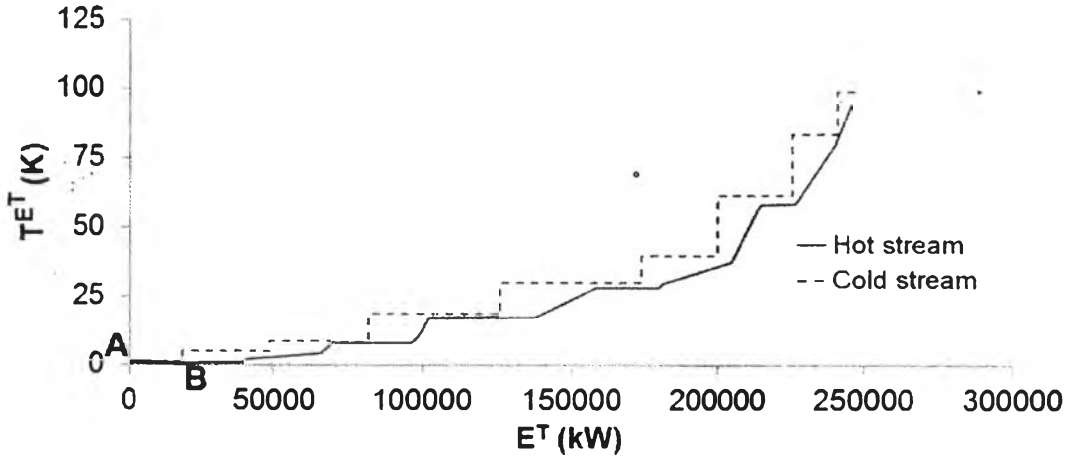

Figure 4.14 Exergy diagram for the alternative 1C multistage cascade refrigeration of LNG process.

Table 4.5 Comparison the methodology to estimate exergy destruction

	Exergy Destruction (kW)	Error
ProII	30,500.89	-
Shaft work	39,449.06	22.7%
Exergy diagram	33,872.57	11%

4.3 Improved Case by the Mathematical Programming

Refrigeration systems are often required to supply low temperature cooling in chemical processes. The design and optimization procedure have to identify the configurations where save both energy and power consumption. This design uses a simple stage-wise model as shown in Figure 4.15 proposed by Yee and Grossman in 1990 which is the MINLP optimization model apply with case study. It allows streams entering each stage be able to split up in each stage interval and then are mixed at the end of each interval with assuming isothermal mixing. In case study, the model is MILP due to without consideration of area terms.

Table 4.6 The stream data for Mathematical optimization

	T_s (°C)	T_t (°C)	T_s (K)	T_t (K)	Q (kW)	FC_p (kW/K)
H1	30	-1.516	303.15	271.634	8300	263.358
H2	-1.516	-23.57	271.634	249.582	6020	272.991
H3	-23.568	-36.17	249.582	236.977	3608	286.236
H4	-36.173	-65.7	236.977	207.45	10378	351.475
H5	-65.7	-86.98	207.45	186.17	31510	1480.73
H6	-86.98	-90.11	186.17	183.036	4000	1276.32
H7	-90.114	-125	183.036	148.15	16100	461.503
H8	-125	-143.7	148.15	129.446	7000	374.251
H9	-143.7	-155	129.446	118.15	4000	354.108
H10	35.801	25.43	308.951	298.58	232300	22399
H11	12.341	-1.36	285.491	271.79	184232	13446.6
H12	-12.311	-23.57	260.839	249.58	141400	12558.8
H13	-23.629	-36	281.75	237.15	140600	3152.47
H14	-35.571	-65.73	248.822	207.416	103700	2504.47
H15	-75.082	-86.94	198.068	186.214	34400	2901.97
H16	-86.9	-90.57	232.016	182.579	51240	1036.47
H17	-89.091	-125.2	184.059	147.941	14831	410.626
H18	-125	-143.6	162.963	129.501	5000	149.423
C1	-4.357	-3.857	268.793	269.293	198100	396200
C2	-26.58	-26.08	246.57	247.07	160032	320063
C3	-38.952	-38.45	234.198	234.698	129400	258800
C4	-68.704	-68.2	204.446	204.946	110600	221200
C5	-89.962	-89.46	183.188	183.688	86400	172800
C6	-93.235	-92.74	179.915	180.415	32800	65600
C7	-128.21	-127.7	144.942	145.442	31200	62400
C8	-146.63	-146.1	126.521	127.021	11650	23300
C9	-161.56	-161.1	111.587	112.087	3915	7830

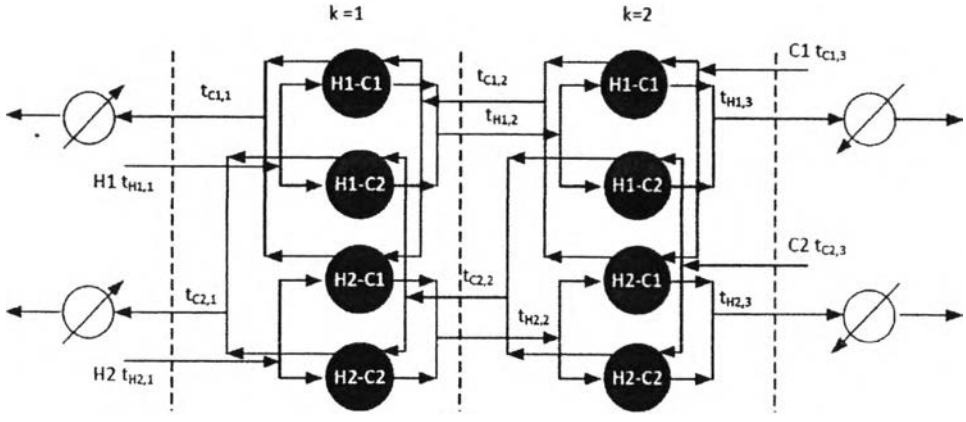

Figure 4.15 A simple stage-wise model (Yee and Grossman, 1990).

Mathematical optimization models for heat exchanger network synthesis rely on the assumptions of: (1) Constant heat capacity flowrates; (2) Fixed inlet and outlet temperatures; (3) Single-pass countercurrent heat exchangers; (4) Layout and pressure drop costs are neglected; (5) Operating cost is given in terms of the heat duties of utilities.

The procedure starts with collect data from base case study, namely inlet temperature, outlet temperature, duty of each stream and heat capacity flowrate of each stream as shown in Table 4.6 and Figure 4.16. The name of streams mention above are defined new names due to it is easy for observation. To overcome a restriction simply in isothermal synthesis because of latent heat by assuming 0.5 °C temperature difference of cold streams. Due to reduction of power consumption depend on the temperature difference of compressor, outlet temperature of compressor ($TH_{i,IN}$) defines to variable as shown in Figure 4.17.

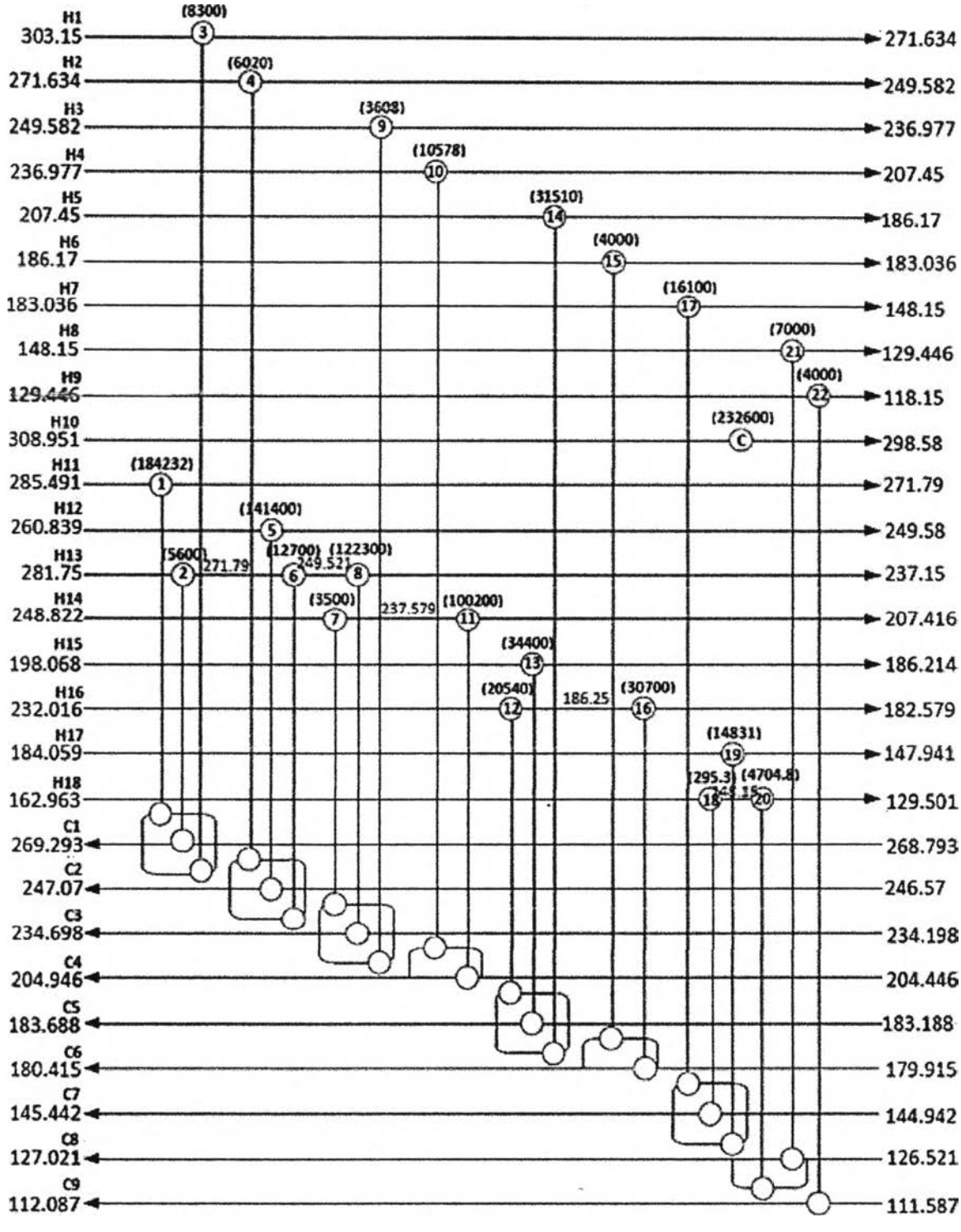

Figure 4.16 HEN of base case multistage cascade refrigeration of LNG process.

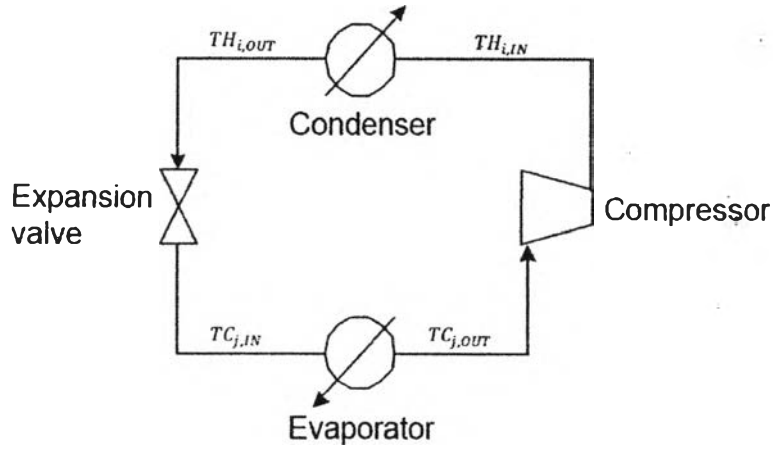

Figure 4.17 A simple refrigeration cycle.

4.3.1 Heat Exchanger Network Synthesis

HEN is designed by applying mathematical programming formulated by objective function with equality and inequality constraints.

Indices and Index Sets

Let i represent hot streams and j represent cold streams.

H $\{ i \mid i$ is hot process stream$\}$

C $\{ j \mid j$ is cold process stream$\}$

K Stage or temperature location; stages are numbered from 1 to ST with descending temperature; for stage k there are two temperature locations, k at inlet and $k + 1$ at outlet

CU $\{ cu \mid cu$ is cooling utility$\}$

Model parameters

$TH_{i,OUT}$ Target temperature of hot process stream i

$TC_{j,IN}$ Supply temperature of cold process stream j

$TC_{j,OUT}$ Target temperature of cold process stream j

$TCUcu_{,IN}$ Inlet temperature of cooling utility cu

$TCU_{cu,OUT}$ Outlet temperature of cooling utility cu

FH_i Heat capacity of hot process stream i

FC_i Heat capacity of cold process stream j

$FW_{i,j}$ Heat capacity of stream between compressor $i-j$

CCU_i Cost of cooling utility cu

CHU_j Cost of heating utility

$CW_{i,j}$ Cost of work consumption of compressor

$CFHX_{i,j}$ Fixed charges for exchanger$i-j$

Ω Upper bound of heat content for heat exchanger

Γ Upper bound for temperature difference $EMAT$ Minimum-approach temperature difference

ST Number of stage (often chosen as maximum between number of hot and cold streams)

Model (Free) variable

$TH_{i,IN}$ Supply temperature of hot process stream i

TAC Total cost associated in heat exchanger network

W Approximately shaft work

Model (positive) variables

$th_{i,k}$ Temperature of hot process stream i at "hot end" of stage k

$tc_{j,k}$ Temperature of cold process stream j at "hot end" of stage k

$q_{i,j,k}$ Heat exchanged between hot process stream $i$and cold process stream j in stage k

$qcu_{i,cu}$ Heat exchanged between cold utility cu and hot process stream i

qhu_j Heat exchanged between hot utility and cold process stream j

$dt_{i,j,k}$ Temperature approach for match $i-j$ at the left of heat exchanger

$dtcu_{i,cu}$ Temperature approach for match between cooling utility cu and hot process stream i

$dthu_j$ Temperature approach for match of heating utility and cold process stream j

Model (binary) variables

In order to define the existence or non-existence of a match in a HEN it is necessary to use binary variables.

$z_{i,j,k}$ Existence of an exchanger for match $i-j$ in stage k

$zcu_{i,cu}$ Existence of an exchanger for match between cooling utility cu and hot process stream i

zhu_j Existence of an exchanger for match between heating utility and cold process stream j

Model Formulation for HEN Synthesis

The HENS objective of minimum TAC is given by

$$Minimize\ (TAC) = \{ [\sum_{i,j,k}(z_{i,j,k}CFHX_{i,j}) + \sum_{i,cu}(zcu_{i,cu}CFCU_{i,cu}) + \sum_{j}(zhu_jCFHU_j)] + [\sum_{i,cu}(qcu_{i,cu}CCU_{i,cu}) + \sum_{j}(qhu_jCHU_j)] + [\sum_{i,j}(WCW_{i,j})]\};$$

$$i \in I, j \in J, k \in ST,\ cu \in CU \tag{4.2}$$

- Overall energy balance of hot and cold streams

Hot: $FH_i(TH_{i,IN} - TH_{i,OUT}) = \sum_{k,j}(q_{i,j,k}) + \sum_{cu} qcu_{i,cu}$;

$$i \in I, j \in J, k \in ST, cu \in CU \tag{4.3}$$

Cold: $FC_j(TC_{j,OUT} - TC_{j,IN}) = \sum_{k,i}(q_{i,j,k}) + qhu_j$;

$$i \in I, j \in J, k \in ST \tag{4.4}$$

- Energy balance at each stage

Hot: $FH_i(th_{i,k} - th_{i,k+1}) = \sum_j(q_{i,j,k})\ ;\ i \in I, j \in J, k \in ST$ (4.5)

Cold: $FC_j(tc_{j,k} - tc_{j,k+1}) = \sum_i(q_{i,j,k})\ ;\ i \in I, j \in J, k \in ST$ (4.6)

- Heat load of cooling utility and heating utility

Cold utility: $\sum_{cu} qcu_{i,cu} = FH_i(th_{i,k} - TH_{i,OUT})$;

$$i \in I, j \in J, k \in ST_{last},\ cu \in CU \tag{4.7}$$

Hot utility: $qhu_j = FC_j(TC_{j,OUT} - tc_{j,k})$;

$$i \in I, j \in J, k \in ST_{first}, hu \in HU \tag{4.8}$$

The cooler is located at the lowest temperature region where is the exit of the superstructure to cool down the hot process stream. The heater is placed at the highest temperature region to heat up the cold process stream at the exit of superstructure.

- Assignments of inlet and outlet temperatures to the superstructure

Hot: $th_{i,k} = TH_{i,IN};\ i \in I, j \in J, k \in ST_{first}$ (4.9)

Cold: $tc_{j,k} = TC_{j,IN};\ i \in I, j \in J, k \in ST_{last}$ (4.10)

The temperature of stream entering to the superstructure should be equal to the supply temperature of that stream. In other words, the temperature of hot stream with $k = ST_{first}$ equals to its supply temperature and the temperature of cold stream with $k = ST_{last}$ equals to supply its supply temperature.

- Constraints ensuring feasibility of temperatures in the superstructure.

Hot: $th_{i,k} \geq TH_{i,OUT}\ ;\ i \in I, j \in J, k \in ST_{last}$ (4.11)

$th_{i,k} \geq th_{i,k+1}\ ;\ i \in I, j \in J, k \in ST$ (4.12)

Cold: $tc_{j,k} \leq TC_{j,OUT}\ ;\ i \in I, j \in J, k \in ST_{first}$ (4.13)

$tc_{j,k} \geq tc_{j,k+1}\ ;\ i \in I, j \in J, k \in ST$ (4.14)

In contrast to the assignment of inlet temperature to the superstructure in equation (4.9) and (4.10), the outlet temperature for some or all streams will be heated up or cooled down by heating or cooling utility. Thus, the inequality relation is required to apply as equation (4.11) and (4.13. Ensuring the feasible temperatures in the superstructure, the constraints of equation (4.12) and equation (4.13) impose that the outlet temperature of any stage is equal to or less than that of previous one. Since heat load in a stage can be zero in case of no heat exchange.

- Logical constraints on heat loads

Heat load: $q_{i,j,k} \leq \Omega z_{i,j,k};\ i \in I, j \in J, k \in ST$ (4.15)

Cold utility load: $qcu_{i,cu} \leq \Omega zcu_i;\ i \in I, j \in J, k \in ST,\ cu \in CU$ (4.16)

Hot utility load: $qhu_j \leq \Omega zhu_j;\ i \in I, j \in J, k \in ST$ (4.17)

The binary variable is introduced to define the existence of match. If the hot stream i matches cold stream j in stage k, the binary variable equals to one.

- Approach temperatures at temperature locations which are the thermodynamic constraints for matches.

Hot end: $dt_{i,j,k} \leq th_{i,k} - tc_{j,k} + \Gamma\left(1 - z_{i,j,k}\right);$

$i \in I, j \in J, k \in ST$ (4.18)

Cold end: $dt_{i,j,k+1} \leq th_{i,j,k+1} - tc_{j,k+1} + \Gamma\left(1 - z_{i,j,k}\right);$

$i \in I, j \in J, k \in ST$ (4.19)

Cold utility: $dtcu_{i,cu} \leq th_{i,k} - TCU_{cu,OUT} + \Gamma\left(1 - zcu_{i,cu}\right);$

$i \in I, k \in ST_{last}, cu \in CU$ (4.20)

Hot utility: $dthu_j \leq TC_{j,out} - tc_{j,k} + \Gamma\left(1 - zhu_j\right);$

$j \in J, k \in ST_{first}$ (4.21)

The following constraints for approach temperatures are used to activate or deactivate by binary variables. To ensure feasible driving forces for exchangers that is selected in the optimization procedure

- Minimum approach-temperature constraints

$dt_{i,j,k} \geq EMAT;\ i \in I, j \in J, k \in ST, cu \in CU, hu \in HU$ (4.22)

Besides, the temperature approaches should be larger than the given $EMAT$ value which is the minimum approach-temperature to ensure the positive approach temperature for existing matches in stage wise superstructure.

- Approximately shaft work

$W = \sum_{i,j} FW_{i,j}\left(TH_{i,IN} - TC_{j,OUT}\right);\ i \in I, j \in J$ (4.23)

4.3.1.1 The Result of HEN Synthesis

The main objective of the case study is to reduce power consumption and energy consumption so that the cost of power consumption by using proposed model. Assuming highest cost of shaft work requirement in order to attend power consumption more than the others by change of temperature variables to reduce shaft work due to the smaller temperature difference of compressor, the saver cost will obtain. The lower bound of temperature variables set at $TH_{i,out}$ from condenser which follow Carnot cycle. Moreover, modification of HEN configuration reduces energy consumption. The result shows in Figure 4.18.

In order to illustrate the HEN design, the case study is taken. The existing HEN of base case consisting twenty two exchangers, as seen in Figure

4.16, requires 232,600 kW of cooling utility and 144,089.53 kW of shaft work. The result of HEN improved structure is illustrated in Figure 4.18 requiring more match of exchangers which consist of twenty nine exchangers. However, there are no need utilities and shaft work requirement is reduced to 108,548.51 kW. The area for base case and improved case exchangers is shown in Table 4.7 and 4.8 in which using Mathematical Programming provide a good design of heat exchanger configuration, resulting in reduced area in term of lumped parameter with overall heat transfer coefficient. The formulations of area calculation are;

$$Q = UA\Delta T_{lm} \tag{4.24}$$

Where,

$$\Delta T_{lm} = \frac{(T_{h,in} - T_{c,out}) - (T_{h,out} - T_{c,in})}{\ln\left[\frac{(T_{h,in} - T_{c,out})}{(T_{h,out} - T_{c,in})}\right]} \tag{4.25}$$

4.3.1.2 Model Validation by PROII

The result from GAMS is validated with PROII by using the same flowrate of each stream and match of exchangers. In Figure 4.19 is illustrated the result of validation, temperature and duty are changed, additionally, three new cooling utilities are added in structure. However, result of validation compared to base case is reduced to 100,951.92 kW of shaft work requirement and 111,400 kW of cooling duty. The data of result is shown in Table 4.9 and Figure 4.19. There is error of phase change of improved case at target temperature of hot stream when compares with base case as shown in Table 4.9 and 4.10 due to result from GAMS with assumption of heat capacity constant and without consideration of latent heat. In addition, Mathematical Programming does not include equation of thermodynamic. Because of Table 4.9 has the problem in stream C8; it should be vapor phase before entering into compressor. To solve this problem by adding one match of exchanger as shown in Table 4.10 and Figure 4.20. It decreases both shaft work requirement and cooling duty which are 89,986.9 kW and 99,100 kW respectively.

4.3.2 HEN Retrofit

The retrofit model is developed from grassroots model. The addition sets of constraints are added into the grassroots model to consider the network

modifications. Therefore, the model consists of 2 sets of equations; the synthesis and retrofit equations. This work uses the MILP model based on the modified and extended Synheat model that proposed for HEN synthesis in the section 4.3.1.

Model Formulation for HEN Retrofit

$$Minimize\ (TAC) = \{ [\sum_{i,j,k} (z^{new}_{i,j,k} CFHX_{i,j}) + \sum_{i,cu} (zcu_{i,cu} CFCU_{i,cu}) + \sum_{j} (zhu_j CFHU_j)] + [\sum_{i,cu} (qcu_{i,cu} CCU_{i,cu}) + \sum_{j} (qhu_j CHU_j)] + [\sum_{i,j} (WCW_{i,j})] \};$$

$$i \in I, j \in J, k \in ST,\ cu \in CU \tag{4.26}$$

The additional constraints are required in retrofit formulation.

- Constraints for existing heat exchanger location

$$z^{EXIST}_{i,j,k} = 1; i \in I, j \in J, k \in ST \tag{4.27}$$

- Constraints for the new process exchangers which the integer variables are 20 for case 1 or 10 for case 2.

$$z^{new}_{i,j,k} = z_{i,j,k} - z^{EXIST}_{i,j,k}; i \in I, j \in J, k \in ST \tag{4.28}$$

$$z^{new}_{i,j,k} \leq integer\ variables\ ;\ i \in I, j \in J, k \in ST \tag{4.29}$$

4.3.2.1 The Result of HEN Retrofit

The objective of grassroots design is to minimize the total cost which includes utilities cost and investment cost of HEN. The aim for retrofit case is to maximize the heat integration among process streams or reduce utilities usage; therefore, maximize the NPV calculated by the energy saving subtracted by the investment cost. Figure 4.16 present the original HEN for base case consisting of 27 streams (18 hot and 9 cold process streams) and 23 exchangers (22 process exchangers, 1 cold utility exchanger). The project life is 5 years with 7,335,000 MW of cold utility consumption per year and 4,544,000 MW power consumption per year of original HEN. Modifications in the HEN account for new exchanger addition and area addition or reduction to existing exchangers. Equations (4.30), (4.31), and (4.32) calculate the total cost of new exchanger, area reduction and area addition made to existing exchangers, respectively. The retrofit match for existing from base case is

shown in Figure 4.21 and 4.22. The results of the retrofitted exchanger area compared to original exchanger area are summarized in Table 4.11 and 4.12. The result of new exchangers less than or equal 20 shows in Figure 4.21. The retrofitted HEN of case 1 consists of 20 existing exchanger and 15 new exchangers added to the network. The total retrofitted area of new process exchanger is 4,363.23 m^2. As a result of increased heat recovery, the usages of cold utilities and power consumption are decreased to 2,680.24 MW per year and 3,706,470 MW per year, respectively. The heat recovery improvement in the retrofitted network results in remarkable NPV: The energy savings is over $5,340 million per year, the NPV is $20,200 million. The result of new exchangers less than or equal 10 shows in Figure 4.22. The retrofitted HEN of case 2 consists of 15 existing exchanger and 10 new exchangers added to the network. The total retrofitted area of new process exchanger is 11,056.36 m^2. As a result of increased heat recovery, the usages of cold utilities and power consumption are decreased to 3,659.97 MW per year and 3,765,460 MW per year, respectively. The heat recovery improvement in the retrofitted network results in remarkable NPV: The energy savings is over $5,078 million per year, the NPV is $19,200 million. Although improved case in case 2 requires less exchangers than case 1, improved case in case 1 provides more total cost saving which presents by higher NPV.

Exchanger cost ($) $= 26{,}460 + [389 \times \text{Area}\ (m^2)]$ (4.30)

Additional area cost ($) $= 13{,}230 + [389 \times \text{Area}^{add}(m^2)]$ (4.31)

Reduction area cost ($) $= 13{,}230 + [0.5 \times \text{Area}^{red}\ (m^2)]$ (4.32)

Table 4.7 The area in term of lumped parameter with overall heat transfer coefficient of base case multistage cascade refrigeration of LNG process

Hx no.	UA (W/°C)	Hx no.	UA (W/°C)	Hx no.	UA (W/°C)
1	23570	9	500.2	17	1152.4
2	833.77	10	862.49	18	35.027
3	656.68	11	8096.1	19	1064.1
4	586.21	12	1308.6	20	507.76
5	19983	13	4938	21	758.57
6	1240	14	3298.3	22	360.38
7	465.79	15	929.26	C	39686
8	16625	16	7590.7		
	∑ UA (W/°C)				135,048.5

Table 4.8 The area in term of lumped parameter with overall heat transfer coefficient of improved case multistage cascade refrigeration of LNG process

Hx no.	UA	Hx no.	UA	Hx no.	UA	Hx no.	UA
1	502.5	9	108.9	17	280.88	25	33.07
2	742.5	10	653.3	18	2222.3	26	3346
3	5608	11	2038	19	174.01	27	130.3
4	5785	12	101	20	263.68	28	0.138
5	1.121	13	347.4	21	91.816	29	23.16
6	2807	14	1.781	22	21.927		
7	310.4	15	389	23	34.146		
8	217.3	16	780.4	24	12807		
	∑ UA (W/°C)				39,834.8		

Table 4.9 The result of HEN validation from Mathematical programming

Stream	Type	Liquid fraction of Improved case	Liquid fraction of base case
H1	NG	0	0
H2	NG	0	0
H3	NG	0	0
H4	NG	1	0.02
H5	NG	1	1
H6	NG	1	1
H7	NG	1	1
H8	NG	1	1
H9	NG	1	1
H10	Propane Condensation	0.69	1
H11	Propane Condensation	0.8	1
H12	Propane Condensation	0.56	1
H13	Ethylene Condensation	1	1
H14	Ethylene Condensation	1	1
H15	Ethylene Condensation	0.55	1
H16	Methane Condensation	0.8	1
H17	Methane Condensation	1	1
H18	Methane Condensation	0.066	1
C1	Propane Evaporation	0	0
C2	Propane Evaporation	0	0
C3	Propane Evaporation	0	0
C4	Ethylene Evaporation	0	0
C5	Ethylene Evaporation	0	0
C6	Ethylene Evaporation	0	0
C7	Methane Evaporation	0	0
C8	Methane Evaporation	0.774	0
C9	Methane Evaporation	0	0

Table 4.10 The result of HEN validation's solution

Stream	Type	Liquid fraction of Improve case	Liquid fraction of base case
H1	NG	0	0
H2	NG	0	0
H3	NG	0	0
H4	NG	1	0.02
H5	NG	1	1
H6	NG	1	1
H7	NG	1	1
H8	NG	1	1
H9	NG	1	1
H10	Propane Condensation	0.54	1
H11	Propane Condensation	1	1
H12	Propane Condensation	0.56	1
H13	Ethylene Condensation	1	1
H14	Ethylene Condensation	1	1
H15	Ethylene Condensation	0.55	1
H16	Methane Condensation	0.81	1
H17	Methane Condensation	0.78	1
H18	Methane Condensation	0.066	1
C1	Propane Evaporation	0	0
C2	Propane Evaporation	0	0
C3	Propane Evaporation	0	0
C4	Ethylene Evaporation	0	0
C5	Ethylene Evaporation	0	0
C6	Ethylene Evaporation	0	0
C7	Methane Evaporation	0	0
C8	Methane Evaporation	0	0
C9	Methane Evaporation	0	0

Table 4.11 The retrofitted exchanger area compared to original exchanger area of case 1 (new exchangers ≥ 20)

Hx No.	Match^{New} (Match^{Exist})	A^{Exist}	A^{New}	(A$^{add/Red}$)
1	H11C1(H11C1)	23,569.98	14,245.20	-9,324.78
2	H13C1(H13C1)	833.77	525.41	-308.37
3	H1C1(H1C1)	656.68	648.60	-8.08
4	H2C2(H2C2)	586.21	586.21	0
5	(H12C2)	19,982.88	20,896.83	+913.95
6	H13C2(H13C2)	1,239.99	548.82	-691.17
7	0(H14C3)	465.79	0	-465.79
8	H13C3(H13C3)	16,624.98	7,677.37	-8947.61
9	H3C3(H3C3)	500.20	477.74	-22.46
10	H4C4(H4C4)	862.49	846.18	-16.32
11	H14C4(H14C4)	8,096.13	6,078.65	-2,017.48
12	0(H16C5)	1308.56	0	-1308.56
13	H15C5(H15C5)	4,938.02	4,696.50	-241.52
14	H5C5(H5C5)	3,298.35	113.25	-3185.09
15	H6C6(H6C6)	929.26	929.23	-0.02
16	H16C6(H16C6)	7,590.73	861.74	-6,728.99
17	H7C7(H7C7)	1,152.37	1,147.34	-5.03
18	0(H18C7)	35.03	0	-35.03
19	H17C7(H17C7)	1064.05	35.64	-1,028.41
20	H18C8(H18C8)	507.76	13.02	-494.75
21	H8C8(H8C8)	758.57	755.72	-2.85
22	H9C9(H9C9)	360.38	347.42	-12.96
23	0(H10CU1)	39,686	0	-39,686

Hx No.	Match^{New} (Match^{Exist})	A^{Exist}	A^{New}	(A$^{add/Red}$)
1'(New)	H10C1	-	3,127.26	+3,127.26
2'(New)	H10C3	-	429.03	+429.03
3'(New)	H1C8	-	0.29	+0.29
4'(New)	H3C8	-	0.57	+0.57
5'(New)	H10C4	-	255.84	+255.84
6'(New)	H10C5	-	184.29	+184.29
7'(New)	H5C8	-	20.38	+20.38
8'(New)	H10C6	-	209.71	+209.71
9'(New)	H10C7	-	97.01	+97.01
10'(New)	H13C8	-	1.37	+1.37
11'(New)	H14C8	-	0.93	+0.93
12'(New)	H16C8	-	6.23	+6.23
13'(New)	H17C8	-	0.02	+0.02
14'(New)	H11C2	-	1.60	+1.60
15'(New)	H18C8	-	16.12	+16.12
CU1(New)	H9CU10	-	12.57	+12.57

Table 4.12 The retrofitted exchanger area compared to original exchanger area of case 2 (new exchangers ≥ 10)

Hx No.	Match^{New} (Match^{Exist})	A^{Exist}	A^{New}	(A$^{add/Red}$)
1	0(H11C1)	23,569.98	0	-
2	0(H13C1)	833.77	0	-833.77
3	H1C1(H1C1)	656.68	0.12	-656.55
4	H2C2(H2C2)	586.21	586.21	0
5	(H12C2)	19,982.88	19,982.74	-0.14
6	H13C2(H13C2)	1,239.99	538.27	-701.73
7	0(H14C3)	465.79	0	-465.79
8	H13C3(H13C3)	16,624.98	191.73	-
9	H3C3(H3C3)	500.20	61.49	-438.71
10	H4C4(H4C4)	862.49	846.18	-16.32
11	H14C4(H14C4)	8,096.13	6,724.14	-1371.99
12	0(H16C5)	1,308.56	0	-1308.56
13	H15C5(H15C5)	4,938.02	4,664.56	-273.46
14	H5C5(H5C5)	3,298.35	116.66	-3181.69
15	H6C6(H6C6)	929.26	929.25	0
16	0(H16C6)	7,590.73	0	-7590.73
17	H7C7(H7C7)	1,152.37	1,156.01	+3.65
18	0(H18C7)	35.03	0	-35.03
19	0(H17C7)	1,064.05	0	-1064.05
20	H18C8(H18C8)	507.76	300.50	-207.26
21	H8C8(H8C8)	758.57	750.70	-7.87
22	H9C9(H9C9)	360.38	346.98	-13.40
23	0(H10CU1)	39,686.32	0	-

Hx No.	Match^{New} (Match^{Exist})	A^{Exist}	A^{New}	(A$^{add/Red}$)
1'(New)	H11C3	-	1,984.60	+1,984.60
2'(New)	H1C7	-	58.67	+58.67
3'(New)	H3C7	-	28.66	+28.66
4'(New)	H13C5	-	806.70	+806.70
5'(New)	H5C6	-	2,118.07	+2,118.07
6'(New)	H17C8	-	80.24	+80.24
7'(New)	H18C9	-	0.17	+0.17
8'(New)	H14C7	-	1.20	+1.20
9'(New)	H16C7	-	100.37	+100.37
10'(New)	H10C1	-	5,863.12	+5,863.12
CU1(New)	H8CU10	-	1.56	+1.56
CU2(New)	H9CU10	-	13.00	+13.00

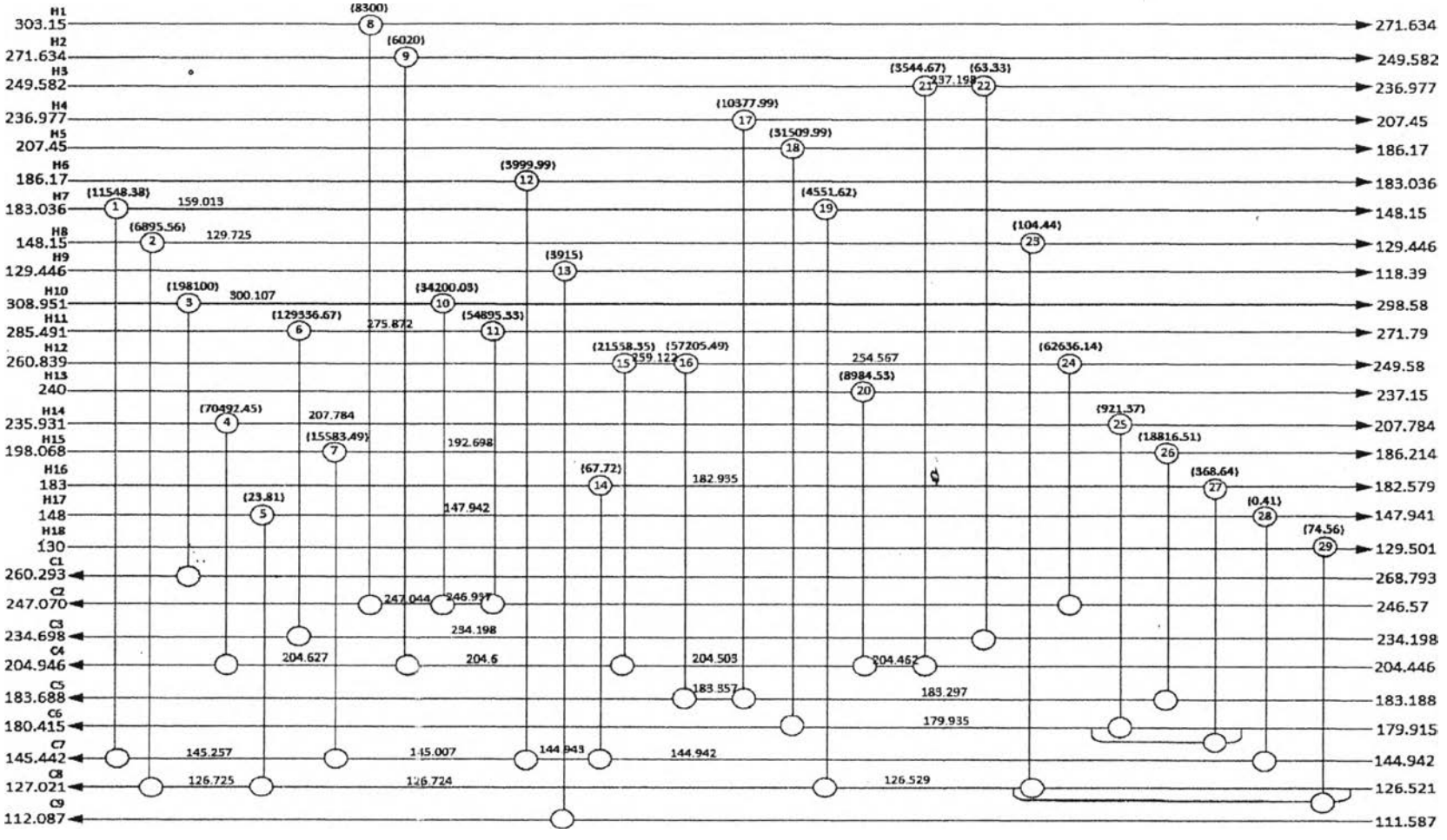

Figure 4.18 HEN of improved case multistage cascade refrigeration of LNG process from Mathematical programming.

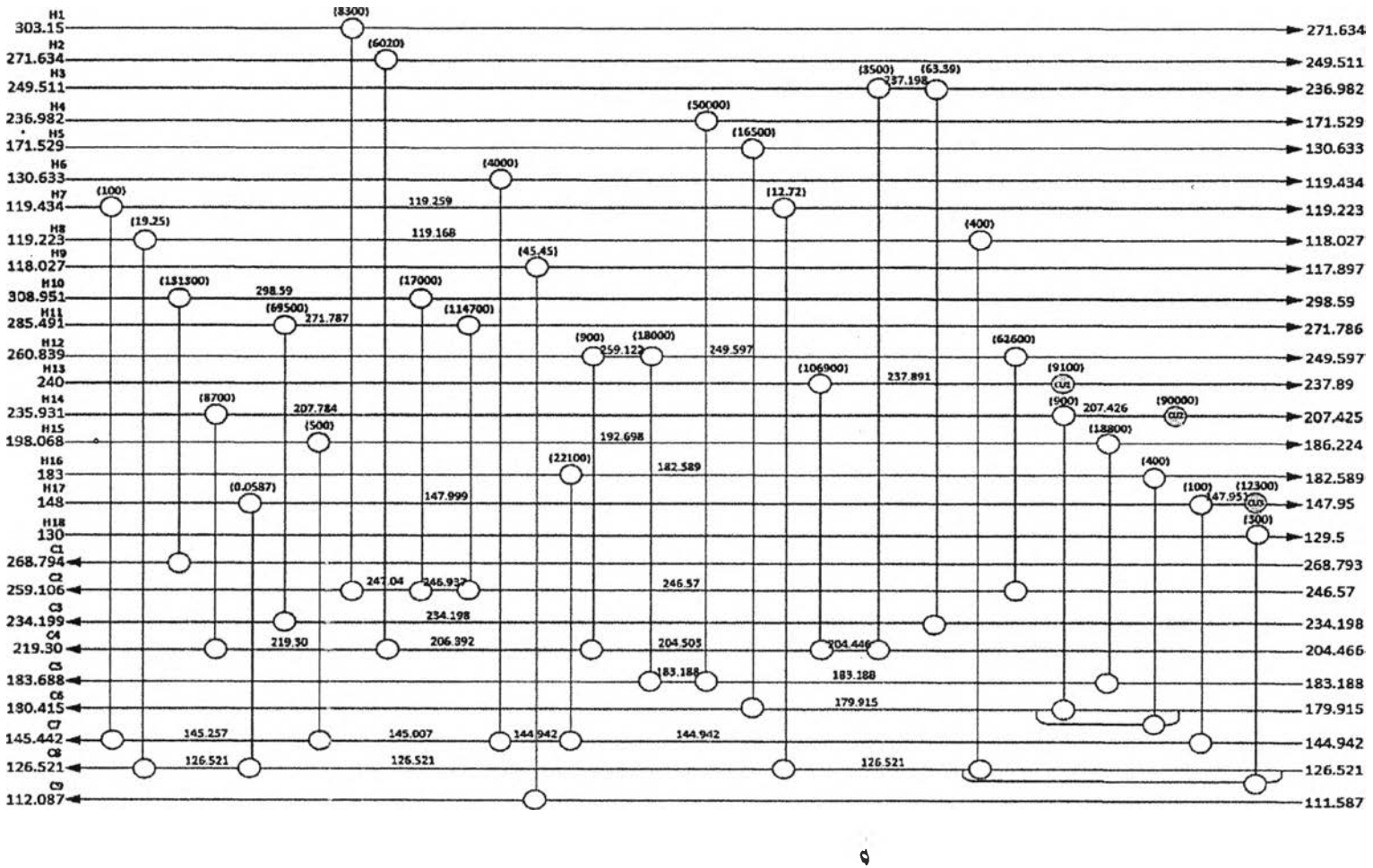

Figure 4.19 The result of HEN of improved case validation from Mathematical programming.

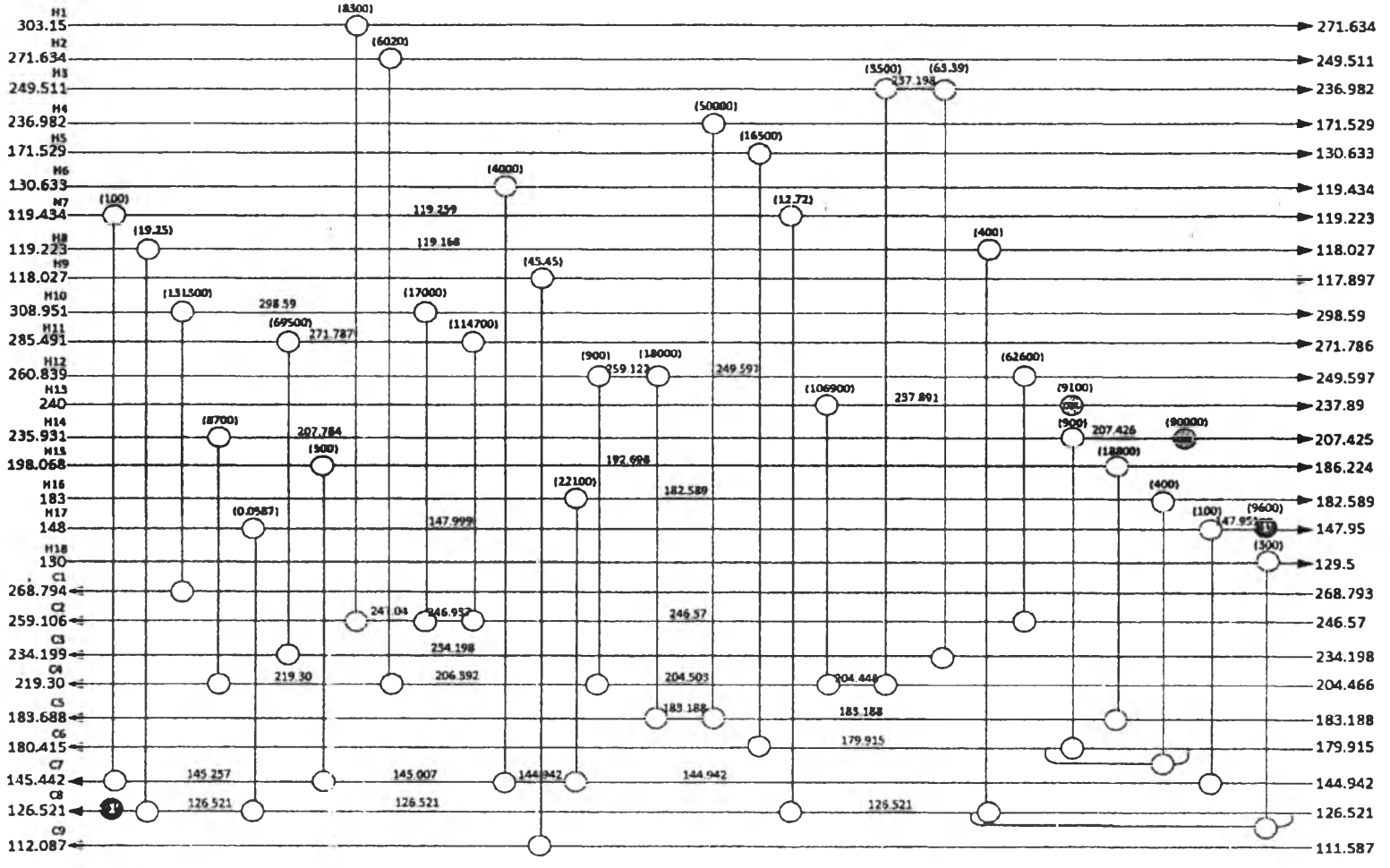

Figure 4.20 The result of HEN of improved cased validation's solution.

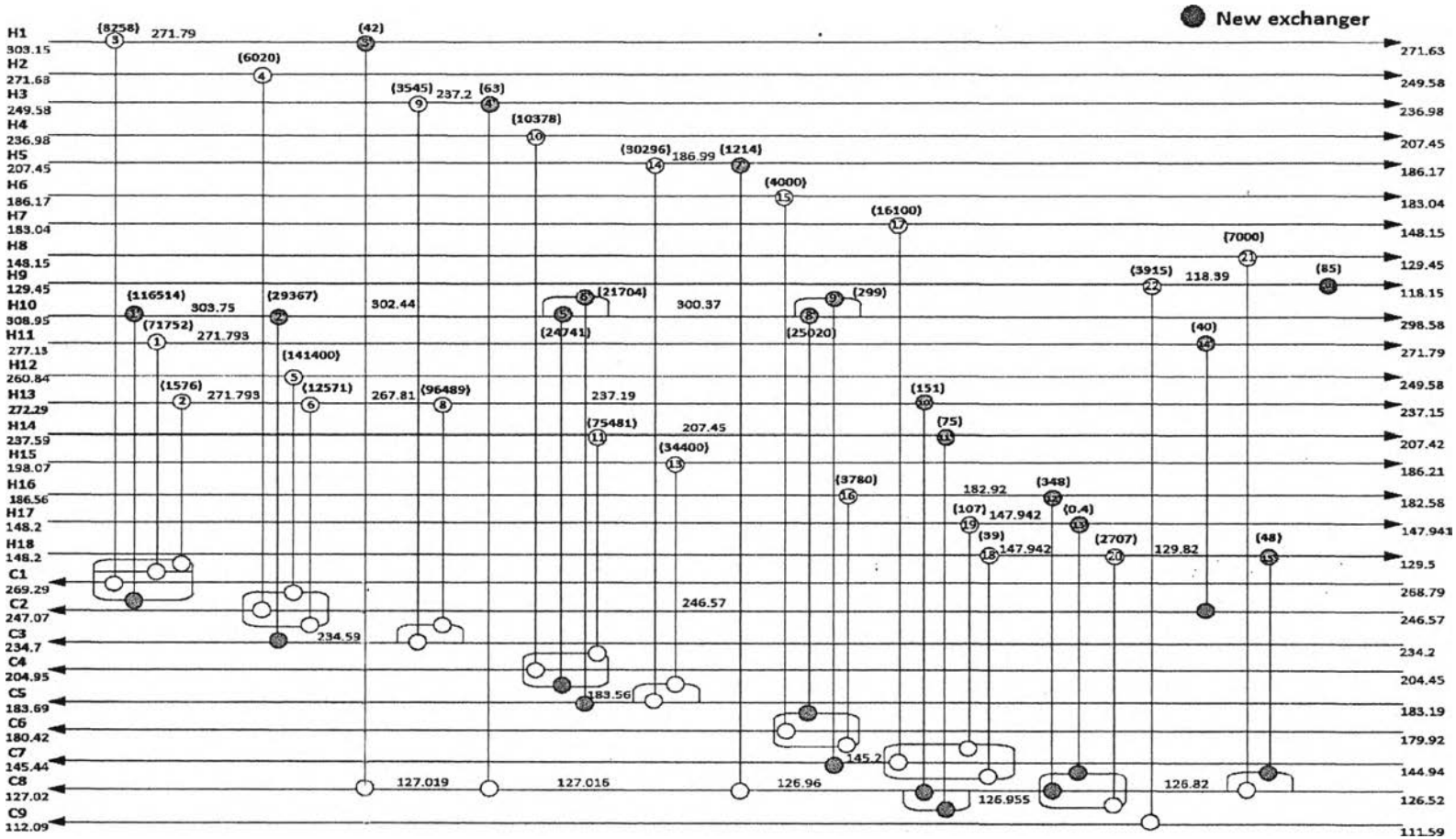

Figure 4.21 The result of retrofitted HEN of case 1 (new exchangers $\geq$ 20).

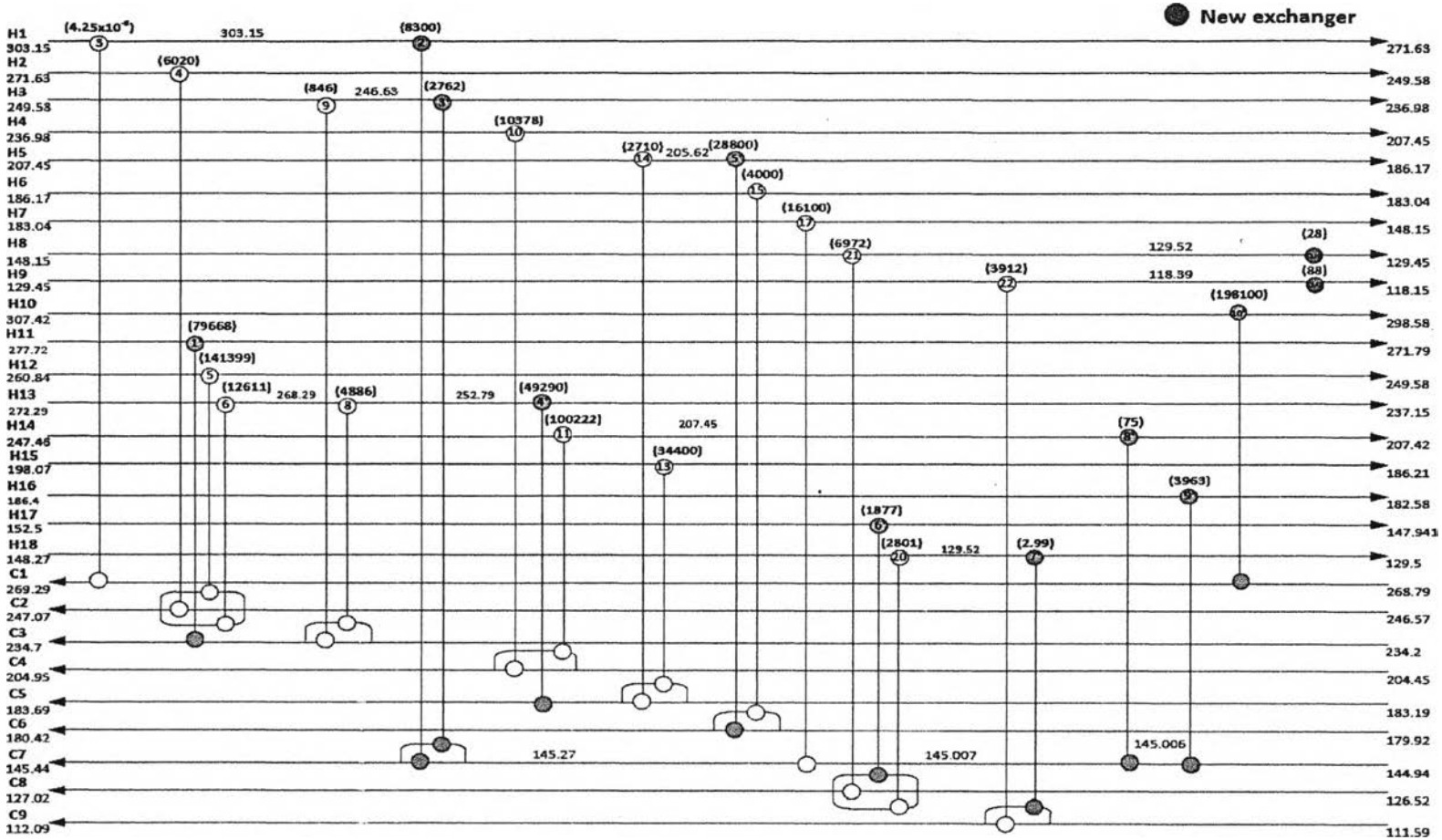

Figure 4.22 The result of retrofitted HEN of case 2 (new exchangers $\geq$ 10).